Journal of Structural Geology, Vol. 6, No. 6, pp. 687 to 692, 1984
Printed in Great Britain

0191-8141/84 $03.00 + 0.00

Comparison of neutron and X-ray diffraction in texture analysis of deformed carbonate rocks

H. R. WENK

Department of Geology and Geophysics, University of California, Berkeley, CA 94720, U.S.A.

H. KERN

Mineralogisch-Petrographisches Institut, Universität, 2300 Kiel, W. Germany

W. SCHAEFER and G. WILL

Mineralogisches Institut, Universität, 5300 Bonn, W. Germany

(*Received* 1 *July* 1983; *accepted in revised form* 28 *December* 1983)

Abstract—The paper compares pole figure determinations with neutron diffraction and X-ray diffraction on experimentally deformed carbonate rocks, a coarse grained marble and fine grained limestone. Neutron diffraction enables determination of complete pole figures on a single spherical specimen and is advantageous for coarse grained materials. Results obtained with both diffraction techniques agree satisfactorily, although uncertainties introduced by counting statistics are more serious for neutrons than for X-rays. Continuous detectors add new possibilities which are still little explored.

INTRODUCTION

PREFERRED orientation of crystals in rocks is generally determined with the universal-stage microscope or by X-ray diffraction. There are limitations in X-ray diffraction which are due mainly to the high absorption of X-rays by matter. Most of the pole-figure measurements are done on flat slabs in reflection or transmission geometry and yield incomplete pole figures with only a relatively small number of grains being recorded. Some of the limitations which exist in X-ray diffraction do not occur for neutrons. Neutron diffraction was applied as early as 1953 for pole figure determinations (Brockhouse 1953) and has since then been used occasionally by metallurgists (for a review see, e.g. Bunge 1982, Feldmann *et al.* 1980). There are also a few studies on geological samples (e.g. Bouchez *et al.* 1979, Bunge *et al.* 1982, Esling *et al.* 1978, Skrotzki & Welch 1983, Wenk *et al.* 1981). In this note we explore some possibilities of neutron diffraction and emphasize quantitative comparisons of neutron and X-ray data obtained on the same samples of experimentally deformed carbonate rocks.

Thermal neutrons have similar energies as X-rays (a Cu (111) monochromator provides a wavelength of λ = 1.289 Å), but their scattering factor is about an order of magnitude smaller (Table 1), requiring long measurements. On the other hand, absorption coefficients for most elements are very small (Table 1), which enables one to use large samples, preferably of roughly spherical shape, with a diameter of up to 2 cm. They are mounted on the same diffractometer used by crystallographers for single-crystal studies, and the full pole figure can be scanned without requiring any corrections. Dimensions of equipment used in neutron diffraction experiments are large compared to X-ray diffractometers (Fig. 1).

Table 1. Comparison of neutron and X-ray scattering factors and absorption coefficients for some common elements

	Scattering factor in 10^{-12} cm*		Mass absorption coefficient in cm^2 g^{-1} †	
	neutron	X-ray ($\theta = 0°$)	neutron ($\lambda = 1.08$ Å)	X-ray (CuKα)
C	0.665	1.69	0.00015	4.60
O	0.580	2.25	0.00001	11.5
Al	0.35	3.65	0.003	48.6
Si	0.42	3.95	0.002	60.6
Ca	0.47	5.6	0.0037	162
Fe	0.95	7.3	0.015	308

* Bacon (1962).
† *International Tables for X-ray Crystallography* (1962).

SAMPLES AND EXPERIMENTS

The samples used in this comparison are experimentally deformed carbonate rocks, a fine grained (<50 μm) micritic limestone from Courrendlin (Swiss Jura) and a coarse grained (1–2.5 mm) marble from Wunsiedel, Fichtelgebirge. Preferred orientation in the starting material is insignificant, at least in the case of limestone. The limestone, specimen 370, was deformed at 200°C, 150 MPa confining pressure, 1.5×10^{-6} s^{-1} strain rate, with $\epsilon_1 = 21.8\%$, $\epsilon_2 = -2.8\%$, and $\epsilon_3 = -20.8\%$. The marble, specimen 376, was deformed at 400°C, 100 MPa confining pressure, 1.6×10^{-6} s^{-1} strain rate, with $\epsilon_1 = 30.2\%$, $\epsilon_2 = -1.4\%$ and $\epsilon_3 = -30.1\%$. Note that deformation approached plane strain in both experiments (compare Kern 1979 and Wagner *et al.* 1982). Neutron diffraction experiments were done at the heavy water moderated research reactor, DIDO, of the K.F.A., Jülich, W. Germany. It provides a flux of monochromatic thermal neutrons at the sample position of about 10^6 n cm^{-2} s^{-1}. The beam size is 20 × 40 mm. Diffracted

neutrons are collimated by Soller slits of variable divergence. This provides a resolution in 2ϑ of 0.3° (measured as full width of diffraction peaks at half maximum and 40° 2ϑ), and divergences on the pole figure of 2° for the pole distance χ and 0.5° for the azimuth φ (at $\chi = 90°$). Diffracted intensities were measured for a preset monitor count-rate (100,000 or 200,000 n), thereby compensating for changes in flux, with a BF_3 detector. The pole figure was scanned along small circles with increments in azimuth $\Delta\varphi$ of 5° for $0° \leq \chi \leq 25°$, 10° for $25° \leq \chi \leq 60°$, and 20° for $60° \leq \chi \leq 90°$ to obtain an equal area coverage of the sphere. Increments in pole distance χ were 5°, giving a total of 757 data points on the hemisphere.

Comparative X-ray measurements were done on a Philips pole figure goniometer with Cu Kα-radiation. Counts on each orientation lasted 1 minute.

RESULTS

Pole figures of the 0006, $10\bar{1}4$ and $11\bar{2}0$ reflections are shown in Figs. 2 and 3.

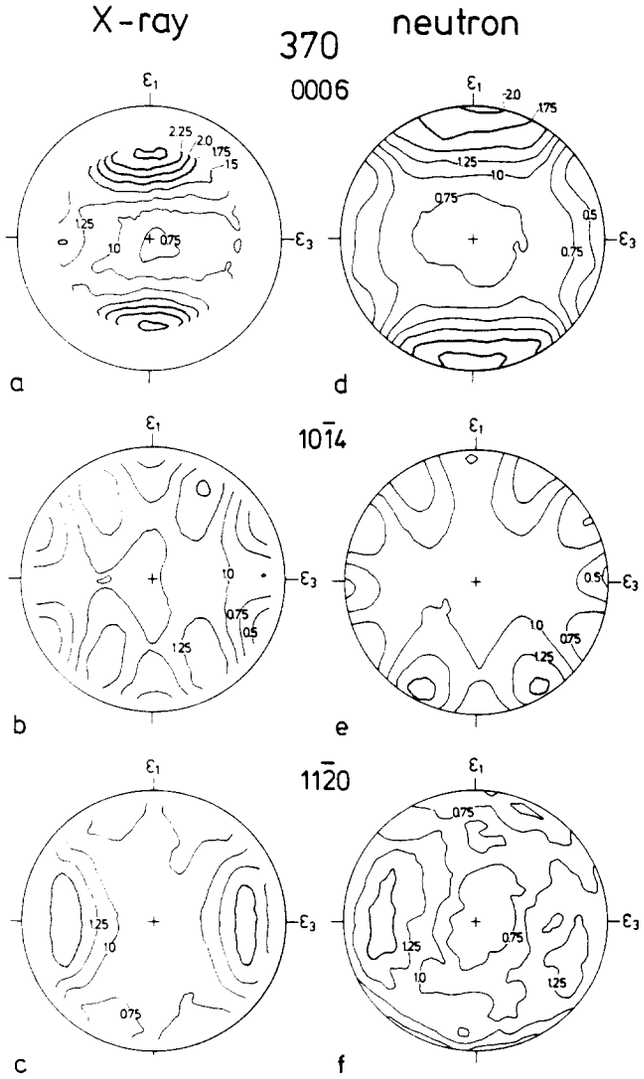

Fig. 2. Comparison of X-ray and neutron pole figures for experimentally deformed limestone 370 (200°C, 150 MPa, $\dot{\epsilon} = 1.5 \times 10^{-6}\,s^{-1}$, $\epsilon_1 = 21.8\%$, $\epsilon_2 = -2.8\%$, $\epsilon_3 = -20.8\%$). Contours are in multiples of a random distribution. Note that the 0006 X-ray pole figure can only be measured to a tilt of $\chi \geq 70°$ due to overlap with the $10\bar{1}4$ reflection.

Table 2. Relative intensities (in 10^{-25} cm^2) of important reflections of calcite with neutron and X-ray scattering. (Scattering factors used are listed in Table 1, intensities are corrected for L_p, assumed wavelength is $\lambda = 1.206$ Å)

hkl	d(Å)	$I_{neutron}$	$I_{X\text{-ray}}$
$01\bar{1}2$	3.868	306	550
$10\bar{1}4$	3.035	912	14346
0006	2.845	301	298
$11\bar{2}0$	2.495	81	2291
$11\bar{2}3$	2.285	379	2218
$20\bar{2}2$	2.095	21	2110

For complex structures, such as calcite, relative structure factors and thus intensities of peaks are in general quite different for X-rays, which scatter on the electrons, and neutrons, which scatter on the nucleus (Table 2). In this respect, the two methods are complementary. The important peak 0006 is strong for neutrons and weak for X-rays. The reverse is true for $11\bar{2}0$ and $20\bar{2}2$.

Compared to X-rays, neutron fluxes are relatively weak. In order to obtain enough intensity, diffraction from at least 10^5 incoming neutrons needs to be counted, resulting in measuring times of 5–15 min for a single position. Even so, the number of counts is generally

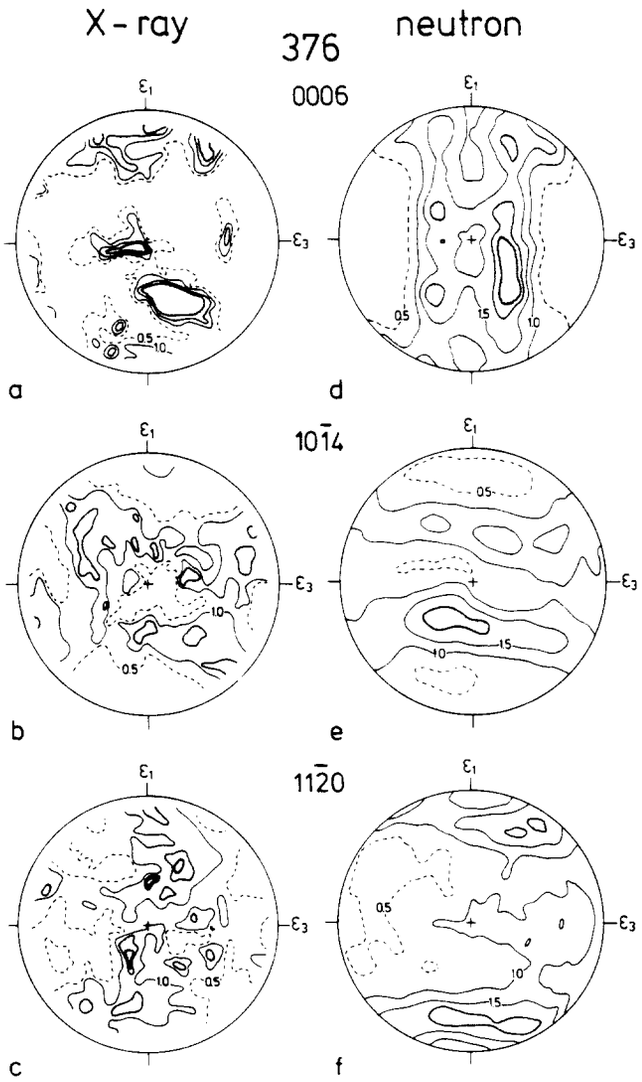

Fig. 3. Comparison of X-ray and neutron pole figures for experimentally deformed marble 376 (400°C, 100 MPa, $\dot{\epsilon} = 1.6 \times 10^{-6}\,s^{-1}$, $\epsilon_1 = 30.2\%$, $\epsilon_2 = -1.4\%$, $\epsilon_3 = -30.1\%$).

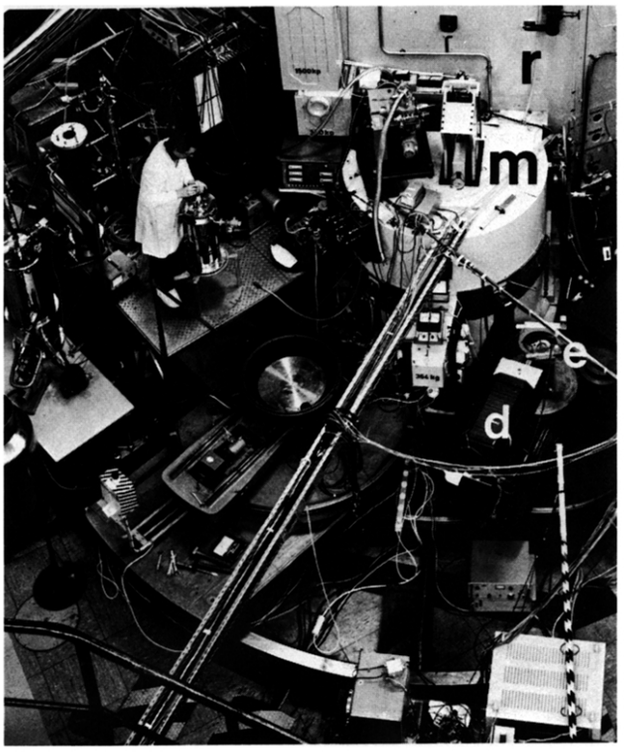

Fig. 1. Photograph of the diffractometer set-up on the reactor DIDO at KFA Jülich during a texture experiment. r, reactor; m, monochromator; e, Eulerian cradle with specimen; d, detector.

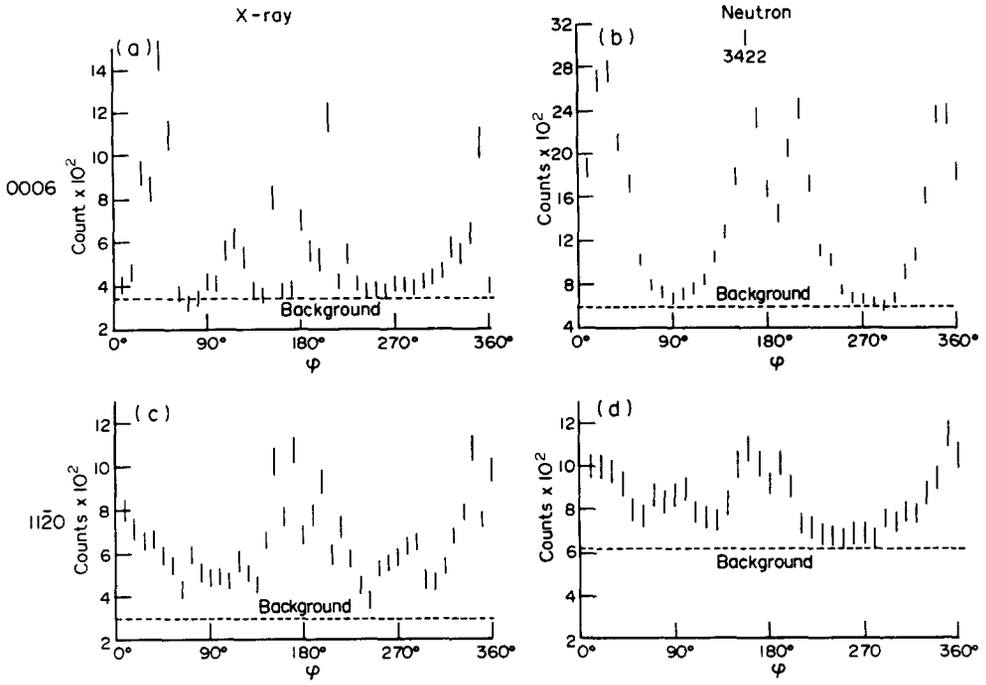

Fig. 4. Intensity profiles for marble sample 376 corresponding to a scan on ϕ in the pole figure at $\chi = 50°$ for 0006 and 11$\bar{2}$0, for X-rays and neutrons. Error bars, based on counting statistics, are $\pm 2\sigma$.

5–10 times lower than in X-ray texture measurements. Furthermore, the background in neutron diffraction is relatively high. Consideration of counting statistics becomes important. This is particularly true for minerals which have weak diffraction peaks. In Fig. 4 we have added to the intensity profile of a section through the pole figure at $\chi = 50°$ values for estimated errors of individual measurements $\pm 2\sigma$ (with $\sigma = \sqrt{I + bg}$ where I is the net intensity and bg the corresponding background). They show that errors of counting statistics are significant in texture determinations, particularly for weak reflections where net intensities are frequently less than 2σ. But texture and sample heterogeneities may outweigh the uncertainties introduced by counting statistics. Figures 2 and 3(a) & (d) compare strong neutron pole figures with weak X-ray pole figures (0006) and Figs. 2 and 3(c) & (f) weak neutron pole figures with strong X-ray pole figures (11$\bar{2}$0). The general texture patterns are similar, even to maximal and minimal values, but resolution in the case of 11$\bar{2}$0 for neutrons is poor.

Neutron diffraction with roughly spherical samples not only eliminates intensity corrections, it also greatly increases the volume of irradiated material, which is crucial for the coarse grained materials found in many rocks. With averaging translation motions, the effective area of X-ray samples can be increased, but even so, practical application is confined to fine grained specimens (grain size < 0.1 mm). The grain size effect is negligible in limestone (Fig. 2) but is considerable in marble (Fig. 3). The effects of grain size are also expressed in intensity profiles. Spikes in Figs. 4(a) & (c) are single crystallites which are generally distorted because not all the intensity enters the receiving slit. A fairly smooth curve is obtained with the neutrons (Figs. 4b & d).

CONCLUSIONS

Application of neutron diffraction offers distinct advantages in texture determinations, particularly for minerals with low angle reflections where intensity corrections for X-rays are most critical. We can measure complete pole figures of coarse grained samples in a single scan. We have described here results from some conventional diffraction experiments on deformed carbonate rocks. Addition of a 2ϑ sensitive continuous detector offers another dimension for simultaneous measurements of the whole spectrum and quantitative deconvolution into single peaks even if peaks in the spectrum are partially overlapped (Bunge *et al.* 1982). Similar possibilities exist with time-of-flight analysis of pulsed neutrons (Feldmann *et al.* 1980). Although access to neutron diffraction sources is limited, structural geologists are encouraged to make use of its excellent potential, particularly for quantitative investigations of texture development. Application of neutron diffraction is easier to justify for minerals than for metals.

An interesting extension of neutron diffraction, not at all explored in the geosciences, is the determination of magnetic pole figures, which has been done in metallurgy (e.g. Henning *et al.* 1981). There are pole figure determinations of magnetite and hematite (e.g. Esling *et al.* 1978, Quade & Walde 1982), but they were interpreted only in terms of crystallographic orientation, and it was not considered that the magnetic moment of Fe contributes an equally important part to the diffracted intensity as scattering on protons and neutrons. Magnetic texture analysis is particularly interesting for crystals with an antiferromagnetic component, where peaks exist in the diffraction pattern which are due solely to magnetic scattering. Pole figures of such peaks may be of significance in paleomagnetic studies.

Acknowledgements—We appreciate access to the neutron source at Jülich and efficient support by their technical staff. Part of the work was done during a sabbatical leave of H.R.W. at the University of Kiel. He acknowledges the hospitality at Kiel and at Bonn, a fellowship from the Alexander von Humboldt Foundation and NSF grant 8207727.

REFERENCES

Bacon, G. E. 1962. *Neutron Diffraction*. Oxford University Press, London.

Bouchez, J.-L., Dervin, P., Mardon, J. P. & Englander, M. 1979. La diffraction neutronique appliquée à l'étude de l'orientation préfèrentielle de reseau dans les quartzites. *Bull. Minéral.* **102**, 225–231.

Brockhouse, B. N. 1953. The initial magnetization of nickel under tension. *Can. J. Phys.* **31**, 339–355.

Bunge, H. 1982. Experimental techniques. In: *Quantitative Texture Analysis* (edited by Bunge, H. J. & Esling, C.). Deutsch. Ges. Metallkunde, Oberursel, 85–128.

Bunge, H. J., Wenk, H. R. & Pannetier, J. 1982. Neutron diffraction texture analysis using a 2θ-position sensitive detector. *Textures and Microstructures* **5**, 153–170.

Esling, C., Wagner, F., Baro, R. & Englander, M. 1978. Textures of iron oxides and topotactical relationships. In: *Textures of Materials* Vol. 2 (edited by Gottstein, G. & Lücke, K.). Springer, Heidelberg, 221–230.

Feldman, K., Betze, M., Andreeff, A., Hennig, K., Kleinstück, K. & Matz, W. 1980. Comparison of quantitative texture analysis results from time-of-flight and conventional neutron diffraction. *Texture of Crystalline Solids* **4**, 1–11.

Hennig, K., Wieser, E., Betzl, M., Feldman, K. & Mücklich, A. 1981. Magnetic texture (magnetic pole figures). In: *Proc. 6th Int. Conf. on Textures of Materials Vol.* **2**, Tokyo, 967–974.

International Tables for X-Ray Crystallography (1962) Vol. 3, Kynoch Press, Birmingham.

Kern, H. 1979. Texture development in calcite and quartz deformed at uniaxial and real triaxial states of strain. *Bull. Minéral.* **102**, 290–300.

Quade, H. & Walde, R. 1982. Texturuntersuchungen an hämatitischen Reicherzen. *Arch. Eisenhüttenwes.* **53**, 85–89.

Skrotski, W. & Welch, P. 1983. Development of texture and microstructure in extruded ionic polycrystalline aggregates. *Tectonophysics* **99**, 47–61.

Wagner, F., Wenk, H. R., Kern, H., Van Houtte, P. & Esling, C. 1982. Development of preferred orientation in plane strain deformed limestone: experiment and theory. *Contr. Miner. Petrol.* **80**, 132–139.

Wenk, H. R., Kern, H. & Wagner, F. 1981. Texture development in experimentally deformed limestone. In: *Deformation of Polycrystals: Mechanisms and Microstructures*. Roskilde, Denmark, Risø National Laboratory, 235–245.